Astron. Astrophys. 343, 297–302 (1999)

ASTRONOMY AND ASTROPHYSICS

New Zr II oscillator strengths and the zirconium conflict in the HgMn star χ Lupi

C.M. Sikström[1], H. Lundberg[2], G.M. Wahlgren[1,3], Z.S. Li[2], C. Lyngå[2], S. Johansson[1], and D.S. Leckrone[4]

[1] Atomic Spectroscopy, Department of Physics, University of Lund, Sölvegatan 14, S-223 62 Lund, Sweden (e-mail: carl_martin.sikstrom@fysik.lu.se)
[2] Atomic Physics, Lund Institute of Technology, Professorsgatan 1, S-223 62 Lund, Sweden
[3] Comp. Sciences Corp., Code 681, GSFC, Greenbelt, MD 20771, USA
[4] Laboratory for Astronomy and Solar Physics, NASA/GSFC, Code 681, Greenbelt, MD 20771, USA

Received 16 September 1998 / Accepted 17 November 1998

Abstract. Lifetimes on the sub-nanosecond scale for the levels $v^2D_{3/2}$, $v^2F_{3/2}$ and $v^2F_{5/2}$ in the 4d5s5p configuration in Zr II have been measured, using the method of laser-induced fluorescence. Combined with branching fractions obtained with the Lund Ultraviolet (UV) Fourier Transform Spectrometer (FTS), experimental oscillator strengths have been derived. From *Hubble Space Telescope*/Goddard High-Resolution Spectrograph spectra, the zirconium abundance in the HgMn star χ Lupi has been determined from Zr II and Zr III lines. More than an order of magnitude difference in the Zr II abundance has been derived from these ionization stages. The difference is much too large to be explained by uncertainties in the oscillator strengths. Possible explanations of this difference have to be found in the stellar models, such as the influence of non-LTE or diffusion.

Key words: atomic data – line: identification – methods: laboratory – stars: abundances – stars: individual: χ Lupi – ultraviolet: stars

1. Introduction

The study of elemental abundances in stellar atmospheres provides evidence for the chemical composition of the stellar primordial cloud, processes occurring within the stellar interior, and the dynamics of the stellar atmosphere. In the case of the chemically peculiar stars of the upper main sequence, tremendous abundance enhancements for many elements are inferred from the observed intensities of spectral lines, and are most often interpreted in terms of diffusion processes in the outer layers of the stellar atmosphere.

A key ingredient in quantitative stellar abundance analyses is the intrinsic atomic line strength, which represents the probability that an atom in a certain state will, through radiative decay or absorption, transfer to another state of lower or higher energy, respectively. The corresponding parameter used in astronomical work is the oscillator strength or *f*-value. The accuracy of the *f*-value for a given transition is critical to the astrophysical interpretation of the observed stellar line since the line area, as measured by its equivalent width, is directly proportional to the product of the *f*-value and the element abundance. Therefore, an error in the *f*-value is directly transferred to the determined abundance, independent of other errors inherent to the analysis.

From the spectrum of the HgMn star χ Lupi it had been noted (Leckrone et al. 1993a,b) that an anomaly existed between the LTE values of the zirconium abundance, as determined from weak lines of Zr II at optical wavelengths and strong Zr III lines detected in the ultraviolet. While such ionization imbalances have been noted for other elements in χ Lupi, the order of magnitude difference in abundance derived from lines of Zr II and Zr III is remarkable. An ionization imbalance of similar magnitude was also noted from lines of Y II and Y III, and investigated further (Brage et al. 1998) in order to determine the role played by *f*-value uncertainties. These elements are part of the Sr-Y-Zr triad, which is vital to the study of s-process nucleosynthesis, and has in the past (Cowley & Aikman 1975) been pointed out as presenting a non-nuclear abundance pattern in HgMn stars. Yttrium and zirconium are often found to be overabundant in HgMn stars by one to three orders of magnitude (Heacox 1979). Observations at ultraviolet wavelengths for lines of the third spectra allow us now to understand that 1) the non-nuclear (odd-even effect) pattern is, in part, the result of mixing abundance data from different ionization stages, and 2) that large ionization imbalances appear to exist for some elements.

The most obvious interpretations for this anomaly may indeed rest with the diffusion theory or the need to account for non-LTE physics. However, a potential lien against any interpretation is the accuracy of the *f*-values for the lines studied. It is this lien we aim to remove by measuring decay lifetimes for energy levels and the branching ratios involved with observed spectral lines of Zr II. We describe our experiments, their results, and application to the observed spectral anomaly in the HgMn star χ Lupi.

Send offprint requests to: C.M. Sikström

2. Branching fractions

Oscillator strengths were determined from measurements of branching fractions (*BF*) and lifetimes. This method is based on the relations

$$BF_{ul} = \frac{\Phi_{ul}}{\sum_l \Phi_{ul}} = \frac{A_{ul}}{\sum_l A_{ul}}$$

and

$$\tau_u = \frac{1}{\sum_l A_{ul}}$$

where $\sum \Phi_{ul}$ and $\sum A_{ul}$ are the sums of the fluxes (in photons·s^{-1}) and the transition probabilities, respectively, from a certain upper level. The flux is measured as an intensity, using a photon counting detection system, for example a photomultiplier tube (PMT). By measuring the lifetime of the upper level, τ_u, one can put the transition probabilities on an absolute scale. From this, *f*-values can be derived.

In order to get the correct *BF*, the intensities of all lines from an upper level have to be observed. Weak lines or lines outside the detector sensitivity region are therefore a problem, which must be dealt with. Weak lines usually contribute less than a few percent of the total branching fraction from an upper level. The strength of weak and unobserved lines can be estimated by performing a calculation.

The FTS is a well suited instrument for these kinds of measurements, as it is able to collect spectral data over a wide region in a single run. Transitions from the *LS* terms of interest in this work, 4d5s5p v^{2}D and 4d5s5p v^{2}F, fall in the region 1740–3600 Å. The strong transitions fall within a narrower region, between 1900–2700 Å, which means that it is possible to measure all such lines in a single spectrum. A solar blind detector, Hamamatsu R166, was used to record the interferogram.

The zirconium spectrum was emitted from a hollow cathode discharge. The cathode was made from a 50 mm long zirconium tube with an inner diameter of 10 mm. A mixture of neon at a pressure of 0.8 torr and argon at 0.2 torr was used as a carrier gas. Neon was used to achieve an effective charge and energy transfer in order to excite the Zr II spectrum, and argon was used for calibration purposes. The spectrum was recorded using the UV FTS in Lund, optimized for use in the UV-region (Thorne et al. 1987). The transmittance of the silica beamsplitter sets the lower wavelength limit at roughly 1750 Å. The reponse of the instrument and the detectors varies with wavelength, and intensity calibration is therefore necessary. The shape of the spectral response was determined from a deuterium lamp having a known intensity curve. The lamp emits a continuous spectrum over the region 1800–3000 Å. Also, known branching fractions of Ar II (Whaling et al. 1993) were used as an internal check, since argon lines originate from the same discharge as the Zr lines and travel an identical light path. The resulting efficiency curve has a sharp cutoff at 3000 Å, which is the upper wavelength limit of the solar blind PMT. The curve peaks at 2500 Å, and falls off to the lower wavelength limit at around 1800 Å, set by the silica beamsplitter and a number of quartz optical components.

Another potential problem is whether or not self absorption is affecting the intensity of strong lines. This effect is most severe for transitions combining down to the ground state, or to levels with low excitation energy. In Zr II, the ground state is a ^{4}D$_{3/2}$ level and the two lowest terms are both quartets. Transitions from the upper terms of interest, 4d5s5p v^{2}D and 4d5s5p v^{2}F, to the quartets are intercombination lines and are forbidden in the LS-coupling scheme. The lowest doublet term has an energy of 4400 cm^{-1}, and therefore has a lower population, which leads us to believe that self absorption has little effect on the line intensities. This conclusion was verified by comparing line intensities of strong and weak lines from the same upper level, when running the hollow cathode lamp at different currents.

The spectrum was analysed using the computer code GREMLIN, which is a development of the computer code DECOMP (Brault & Abrams 1989). The program fits a Voigt function to the observed line. The area under the fitted profile was used as the line intensity. Uncertainties in the calibrated intensities were assumed to arise from statistical and calibration errors. The noise level in a FTS spectrum can be assumed to be constant over the entire spectral region. The signal-to noise ratio (S/N) is therefore only dependent on the observed intensity of a line. Note that a line with a high *f*-value does not necessarily have a high observed intensity due to the wavelength dependence of the instrumental response. The intensity calibration was assumed to be accurate to within 5% at the maximum response of the sensitivity curve. Calibration becomes relatively more uncertain in regions of lower instrumental response, giving lines in the wings of the calibration curve larger uncertainties. The resulting uncertainty thus depends on both the observed intensity and the intensity calibration.

3. Radiative lifetimes

In the lifetime measurements the experimental technique employed a laser-produced plasma, pulsed laser excitation and time-resolved detection. Zirconium ions in the ground level and low-lying metastable levels were created by irradiating a zirconium target with laser pulses. The pulses had an energy of about 25 mJ, a duration of 10 ns and were focused onto the target by a 30 cm focal-length lens. Ions in the expanding plasma were then excited from one of the low levels to the level under investigation by the UV light from a pulsed laser system. Tunable radiation in the region 7000–8000 Å was obtained from a distributed-feedback dye laser. The dye laser was pumped by a part of the output from a mode-locked and Q-switched Nd:YAG laser. The dye laser output was amplified to a few mJ and converted to UV using frequency-mixing crystals. For the high-lying levels of the 4d5s5p configuration the tunable dye-laser output was mixed with the fourth harmonic of the Nd:YAG laser giving the desired excitation wavelengths around 195 nm. The pulse duration was 70 ps, which is much shorter than the measured lifetimes. The excitation beam interacted with the ions about 10 mm above the target. In these measurements the excitation could be performed from low metastable levels, which is favourable for lifetime observations. Whereas the higher metastable levels

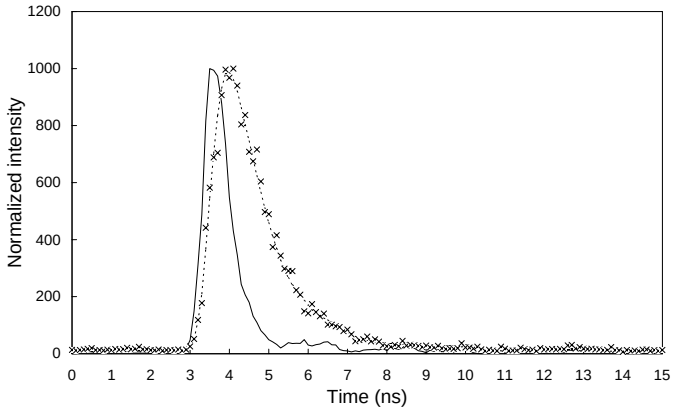

Fig. 1. Lifetimes were measured using the method of laser induced fluorescence. The solid line shows the recorded pulse and the dashed line the fitted fluorescence decay curve. The data points for the fluorescence are marked as x in the figure. The curve was recorded observing the decay from the upper level $v^2D_{3/2}$, and the lifetime was found to be 770(80)ps.

decay rapidly due to collisions and only are present early in the plasma evolution, the lower metastable levels persist to later times when the plasma background-radiation and temperature has diminished.

Fluorescent light was detected in a direction perpendicular to the flight direction of the ions and the direction of the exciting radiation. One decay channel, different from the excitation, was selected using a 0.25 m monochromator. The decay was recorded by a Hamamatsu 1564U micro-channel plate photomultiplier connected to a Textronix Model No DSA 602 digital oscilloscope. A more detailed description of the experimental setup can be found in Larsson et al. (1996). For each lifetime measurement two recordings were made; the dye laser pulse and the fluorescence decay. An example of recorded curves is shown in Fig. 1. The time response of the detection system was mainly limited by the bandwidth of the oscilloscope input amplifier. The finite rise-time of the PMT and signal cables also contributed to limiting the time response. The measured FWHM of the recorded laser pulse is therefore about 1 ns. The lifetime values were obtained in a least-square fit of the recorded fluorescence to a convolution of the recorded laser pulse and an exponential. The lifetime values are given in Table 1. Two levels belonging to the $4d^25p$ configuration were measured for comparison with previous results, reported by Biémont et al. (1981) and Langhans et al. (1995), and a good agreement was obtained.

4. Oscillator strengths

The transition probability, A_{ul}, can be derived by dividing the branching fraction, B_{ul}, with the lifetime of the upper level, τ_u. The transition probability can then be converted into an oscillator strength, *f*, by a numerical factor. Table 2 presents the log *gf*-values. Before deriving the oscillator strength, the intensity of the transitions too weak to be detected must be estimated. A Hartree-Fock calculation was performed, using the Cowan computer code package (Cowan 1981), modified for PC by Ralchenko & Kramida (1995). The configurations $4d^3$, $4d^25s$, $4d^25p$, $4d^26s$, $4d^26p$, $4d5s5p$, $4d5s^2$ and $5s^25p$ were included in the calculation. The wavefunctions used in the final calculations were obtained after a least squares fit of calculated levels to observed energy levels obtained by Kiess & Kiess (1930), Kiess (1953) and Johansson & Nilsson (1996). The theoretical branching fractions were compared with the experimental values and were in most cases found to be in good agreement. The combined theoretical intensity of lines too weak to be detected was on the order of 10% of the total intensity from a given upper level. The sum of the theoretical branching fractions was used to correct the experimental values. This sum is given as the residual in Table 2. The uncertainty in the *f*-values is estimated to be 25% in lines with high observed intensities and no more than 40% in the weakest lines observed. The uncertainty has been estimated for each line individually, and is given in the last column in Table 2.

The Zr III oscillator strengths used in the astrophysical applications of the next section were calculated by Redfors (1991) using the Cowan computer code. Using these oscillator strengths, a zirconium abundance of log N_{Zr}=3.92 (on a scale where log N_H=12.00) has been derived for Zr III lines in the UV region (Leckrone et al. 1998). In a recent paper by Reader & Acquista (1997), oscillator strengths of Zr III transitions were calculated also using the Cowan code. A comparison between these two studies shows no significant difference in the oscillator strengths used in the determination of the Zr abundance by Leckrone et al. (1998). However, in a paper by Brage et al. (1998) the importance of including core polarization in the calculation of *f*-values for the spectra Sr II and Y III was pointed out. The Hartree-Fock values of Brage et al. (1998) agree with the relativistic values of Redfors (1991). Adding the effect of core polarization for Y III, on average the values of Redfors should be scaled down by a factor of 1.4 to account for this effect. A comparison of the Zr III oscillator strengths calculated by Redfors and by Brage (1998) shows the same effect. By analogy, a rough estimate of the effect of including the influence of core polarization in Redfors calculations on Zr III can be made by dividing his *gf*-values by a factor of 1.4. This scaling factor was found by taking an average of the difference between Redfors' and Brage's *gf*-values. This had to be done since only some of the transitions calculated by Redfors were calculated by Brage. In particular, the transitions of interest, in the region 1900–2000 Å were not included by Brage. We estimate the accuracy of the scaled values to be better than 30%. The scale factor of 1.4 in the *f*-value corresponds to an increase in the abundance of appoximately 0.15 dex. This implies that the abundance of Zr in χ Lupi derived by (Leckrone et al. 1998) from Zr III lines in the ultraviolet should be corrected to be 4.07 dex.

5. Astrophysical applications

We have applied the new *f*-values described above to the determination of the zirconium abundance in the cool HgMn star χ Lupi (B9.5VpHgMn + A2Vm) from data obtained using the echelle mode of the Goddard High Resolution Spectrograph

Table 1. Measured lifetimes in Zr II.

Configuration	Level	Energy (cm^{-1})	Excitation (nm)	Lifetime (ns)		
				this work	Langhans et al.	Biémont et al.
$4d^25p$	$z^4G^o_{11/2}$	30796	369.746	5.4(4)	–	–
$4d^25p$	$z^4F^o_{7/2}$	31249	363.645	4.7(3)	-	4.65(20)
$4d^25p$	$z^4D^o_{3/2}$	32257	309.923	6.9(4)	6.9(2)	–
4d5s5p	$v^2D^o_{3/2}$	55834	194.822	0.77(8)	–	–
4d5s5p	$v^2F^o_{5/2}$	57062	194.898	0.88(8)	–	–
4d5s5p	$v^2F^o_{7/2}$	57740	195.034	0.94(9)	–	–

Table 2. Absolute oscillator strengths of Zr II lines. Air wavelengths used above 2000 Å.

Upper Level	Lower Level	Wavelength[a] (Å)	Wavenumber[a] (cm^{-1})	Branching Fraction	log *gf*	Uncertainty[b]
4d5s5p $v^2D^o_{3/2}$	$4d^3\ b^2P_{1/2}$	2760.002	36221.148	0.012	−1.146	C
	$4d^3\ b^2F_{5/2}$	2752.513	36319.700	0.043	−0.599	B
	$4d^3\ c^2D_{5/2}$	2432.282	41101.190	0.006	−1.525	C
	$4d^3\ c^2D_{3/2}$	2406.822	41535.932	0.047	−0.671	B
	$4d5s^2\ b^2D_{5/2}$	2398.983	41671.650	0.019	−1.081	B
	$4d5s^2\ b^2D_{3/2}$	2357.431	42406.088	0.205	−0.052	A
	$4d^25s\ a^2F_{5/2}$	1996.742	50081.576	0.295	−0.038	A
	$4d^25s\ a^2D_{5/2}$	1948.218	51328.948	0.103	−0.517	B
	$4d^25s\ a^2D_{3/2}$	1938.500	51586.279	0.197	−0.239	B
	residual			0.074		
4d5s5p $v^2F^o_{5/2}$	$4d^3\ b^2P_{3/2}$	2703.249	36981.554	0.009	−1.166	C
	$4d^3\ b^2F_{5/2}$	2662.542	37546.930	0.019	−0.859	C
	$4d^3\ c^2D_{5/2}$	2361.757	42328.420	0.038	−0.662	B
	$4d5s^2\ b^2D_{5/2}$	2330.348	42898.880	0.141	−0.106	A
	$4d^25s\ b^2G_{7/2}$	2324.758	43002.023	0.140	−0.111	A
	$4d^25s\ b^2D_{3/2}$	2291.120	43633.318	0.170	−0.040	A
	$4d^3\ a^2G_{7/2}$	2030.870	49224.128	0.055	−0.637	B
	$4d^25s\ a^2F_{7/2}$	1976.513	50594.165	0.074	−0.531	B
	$4d^25s\ a^2F_{5/2}$	1948.983	51308.806	0.183	−0.148	B
	residual			0.171		
4d5s5p $v^2F^o_{7/2}$	$4d^3\ c^2D_{5/2}$	2324.475	43007.259	0.029	−0.698	B
	$4d^25s\ b^2G_{9/2}$	2295.488	43550.310	0.155	+0.019	A
	$4d5s^2\ b^2D_{5/2}$	2294.044	43577.719	0.393	+0.420	A
	$4d^25s\ b^2G_{7/2}$	2288.626	43680.862	0.009	−1.217	B
	$4d^3\ a^2H_{9/2}$	2184.812	45756.214	0.009	−1.257	C
	$4d^3\ a^2G_{9/2}$	2015.971	49587.874	0.076	−0.403	B
	$4d^25s\ a^2F_{7/2}$	1950.344	51273.004	0.123	−0.222	B
	$4d^25s\ a^2D_{5/2}$	1878.463	53235.017	0.114	−0.292	C
	residual			0.092		

[a] Wavelengths and wavenumbers derived from improved energy levels by Johansson.
[b] Uncertainty in the *f*-value. A = ±25%, B = ±30%, C = ±40%.

(GHRS) onboard the *Hubble Space Telescope (HST)*. The generally high data quality can be described by a spectral resolving power of R = $\lambda/\delta\lambda$ = 85000 and a S/N of approximately 100:1. The GHRS observations of χ Lupi comprise a large part of the χ Lupi Pathfinder project (Leckrone et al. 1998), which is an effort to fully characterize the elemental abundance distribution in this star. The high spectral resolution data at ultraviolet wavelengths has required an investment by atomic spectroscopists and astronomers into acquiring wavelength and oscillator strength data of high quality, often involving an accounting for hyperfine and isotopic components. The χ Lupi spectra have also been presented in an atlas format by Brandt et al. (1998) with an accompanying paper (Leckrone et al. 1998) detailing the abundance results to date.

Of the transitions presented in Table 2, seven lie within the GHRS spectral regions obtained for χ Lupi. Of these seven lines, severe line blending or an intrinsically weak nature allow for only three lines (Zr II λ 1938.500, 2357.431, 2324.758 Å) to be

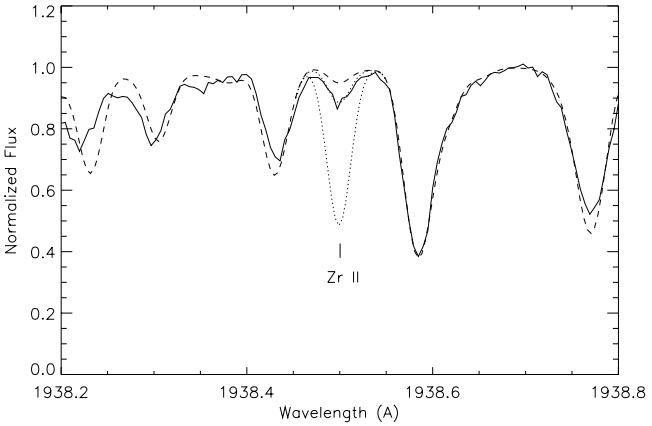

Fig. 2. Zr II λ1938.500 for χ Lupi. The observed spectrum (solid line) is plotted along with synthetic spectrum computed for the the zirconium abundances, log N_{Zr} = 2.60 (solar, dashed line), 2.86 (best fit, dotted), and 3.92 (Zr III best fit, dotted). This GHRS observation has R = 87000, L_A/L_B = 6.58 and $\Delta\lambda_{AB}$ = +0.80 Å.

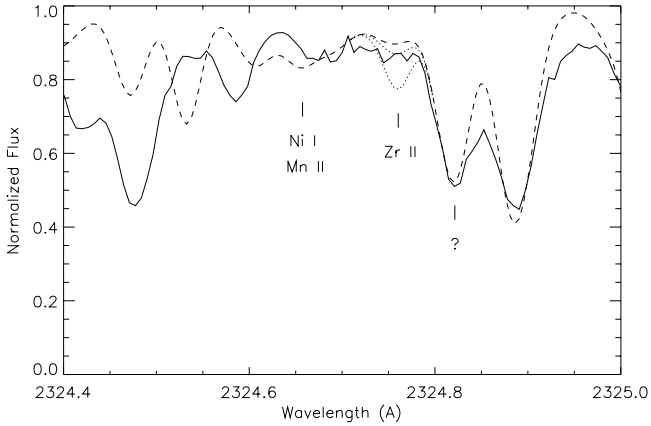

Fig. 3. Zr II λ2324.758 for χ Lupi. An upper limit abundance of log N_{Zr} = 3.26 is obtained from this feature. Figure symbols are as in Fig. 2. The identity of the strong line at 2324.82 Å is unknown but has been modeled to account for absorption in the wing of the Zr II line. For this observation R = 84100, L_A/L_B = 6.08, and $\Delta\lambda_{AB}$ = +0.28 Å.

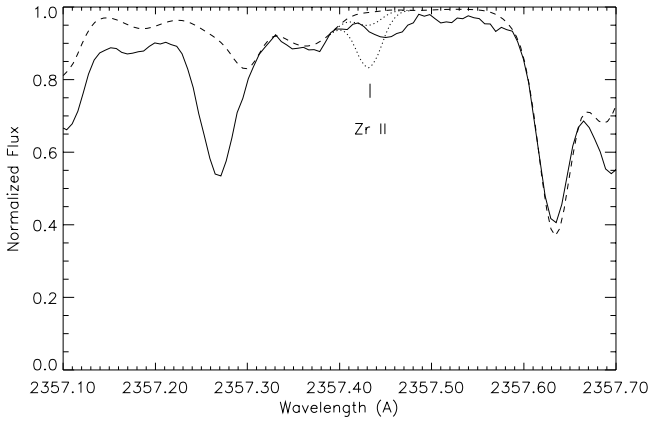

Fig. 4. Zr II λ2357.431 for χ Lupi. The upper limit abundance of log N_{Zr} = 3.26 is obtained for this feature. Figure symbols are as in Fig. 2. For this observation R = 87600, L_A/L_B = 6.06, and $\Delta\lambda_{AB}$ = +0.59 Å.

studied with confidence. Our synthetic spectrum technique has been described in previous abundance analyses. It involves fitting the observed, flux normalized spectra with synthetic spectra generated with the SYNTHE code (Kurucz 1993), and utilizes ATLAS8 model atmospheres generated for stellar parameters as given by Wahlgren, Adelman, & Robinson (WAR, 1994) for both components of the χ Lupi binary system. Synthetic spectra for each of the χ Lupi components were coadded according to the orbital ephemeris of Dworetsky (1972) and the light ratios, L_A/L_B, of WAR.

The line list data is that of Kurucz (1993), with the exception of the Zr II line data presented by this paper and changes made to the line list that address blending issues in the immediate vicinity of the zirconium lines. Line broadening by radiative and collisional processes are accounted for through the semi-empirical formalisms of Kurucz (1993). To our knowledge, neither experimental nor more elaborate calculations of broadening constants specific to the transitions of our study have been carried out. None of the three Zr II lines we are able to study provide meaningful line width information, particularly for the line wings, from which alternative Stark broadening formalisms may be tested.

A thorough examination of line identifications for the wavelength region 1938–1948 Å has been undertaken from the GHRS spectrum of χ Lupi (Leckrone, unpublished) and has been used in this study. The lines of Zr II are represented as single component structures. Although terrestrial zirconium is comprised of five stable isotopes, two of which are of odd atomic number and possess hyperfine structure (hfs), no line broadening has been observed in our laboratory FTS spectra. Therefore, the line broadening mechanisms of hfs and isotopic shifs (IS) are not a concern in our analysis. On the other hand, we do not have the possibility to study the IS that are so important as constraints to diffusion theory.

The results of the synthetic spectrum fitting are presented graphically in Figs. 2, 3 and 4. The figure captions provide details of the observations concerning the spectral resolving power, R = $\lambda/\delta\lambda$, and the wavelength shift, $\Delta\lambda_{AB} = \lambda_A - \lambda_B$, between the binary components at the time of the observation. In each figure the observed spectrum (solid line) is compared against three synthetic spectra representing the zirconium abundances (log N_{Zr}) for cases of the solar abundance (2.60, Anders & Grevesse 1989, dashed line), the best fit to the observed feature (dotted), and the best fit to Zr III lines found in GHRS spectra (4.07, corrected Leckrone et al. 1998, dotted line).

Zr II λ1938.500 provides the most reliable zirconium abundance from among the Zr II lines. This line is unblended and is one of the strongest of the Zr II lines which we have investigated. It is best fit by the value log N_{Zr} = 2.86, which represents a weak zirconium enhancement (+0.26 dex) compared to the 1.47 dex enhancement evident from strong Zr III lines.

The remaining two lines analysed (Zr II λ2324.758, 2357.431) serve to confirm the result from the 1938.500 line. However, due to unresolved line blending issues the abundances derived are considered to be upper limits. For both of these lines

the zirconium abundance must be less than log N_{Zr} = 3.26. For Zr II λ2324.758 the line blending concerns centered around the potential contributions to the line wings by the relatively distant lines Ni I λ2324.654 and Mn II λ2324.664. The original synthetic spectrum (not pictured) produced strong absorption from the Ni I line. Its oscillator strength was reduced from the value found in the Kurucz line list (log gf = +0.009) by an arbitrary amount to the value of log gf = -1.000. This result is presented by Fig. 2. The contribution of this feature at the location of the Zr II line is trivial. An unidentified line(s) exists at the location near 2324.82 Å. We have included a fictitious Fe II line into our line list at this location for the purpose of reproducing the line absorption contribution in the wing of the Zr II line. The results of this calculation show that the Zr abundance based on Zr III produces absorption for Zr II that is significantly greater than the observation.

Absorption at the location of the Zr II λ2357.431 line also suffers from the effects of line blending. We chose not to include fictitious lines into the analysis since the broader nature of the blend indicates multiple line blending with perhaps contributions from the companion star. The zirconium abundance of 3.26 dex produces absorption that attains the depth of the observation and clearly indicates that the abundance from Zr III lines is greater than that afforded by this Zr II line.

6. Conclusions

A conflict in the zirconium abundance derived from lines of Zr II and Zr III in the UV region in the star χ Lupi has been observed. Using the emission method, combining experimental branching fraction measurements with radiative lifetimes, we have derived absolute oscillator strengths for 27 lines of Zr II. Also, Redfors' (1991) theoretical *gf*-values for Zr III lines have been scaled to account for the influence of core polarization which was not taken into account in that calculation.

The application of the new oscillator strength data to the spectra of the HgMn star χ Lupi confirms the earlier ionization imbalance determined from computed oscillator strength data for Zr II lines at ultraviolet wavelengths. The small difference from the earlier work acts to slightly increase the magnitude of the imbalance, which is significantly greater than the uncertainties of the experimental *f*-value determination. We therefore conclude that the LTE abundance difference obtained from different ions is not the result of incorrect *f*-values. The cause of the imbalance must therefore lie in other sources, such as the appropriateness of the stellar model and the effects of non-LTE and diffusion processes.

Acknowledgements. The authors would like to thank Dr. U. Litzén for assistance and guidance especially during the laboratory FTS work. This project is supported by the Swedish National Science Research Council and the Swedish National Space Board. GMW wishes to acknowledge financial support from the Crafoord Foundation.

References

Anders E., Grevesse N.; 1989, Geochim. Cosmochim. Acta 53, 197
Biémont E., Grevesse N., Hannaford P., Lowe R.M., 1981, ApJ 248, 867
Brage T., Wahlgren G.M., Johansson S.G., Leckrone D.S., Proffitt C.R., 1998, ApJ 496, 1051
Brage T., 1998, Private communication
Brandt J.C., Heap S.R., Beaver E.A., et al., 1999, AJ in press
Brault J.W., Abrams M.C., 1989, High Resolution Fourier Transform Spectroscopy. OSA Technical Digest Series, vol. 6, Optical Society of America, Washington, 110
Cowan R.D., 1981, The Theory of Atomic Structure and Spectra. Univ. of California Press, Berkeley
Cowley C.R., Aikman G.C.L., 1975 ApJ 196, 521
Dworetsky M.M., 1972, PASP 84, 254
Heacox W.D., 1979, ApJS 41, 675
Johansson S., Nilsson A.E., 1996, Private communication
Kiess C.C., Kiess H.K., 1930, J. Res. Nat. Bur. Stand. 5, 1205
Kiess C.C., 1953, JOSA 43, 1024
Kurucz R.L., 1993, SYNTHE Synthesis Programs and Line Data. Kurucz CD-ROM No. 18
Langhans G., Schade W., Helbig V., 1995, Z. Phys. D 34, 151
Larsson J., Zerne R., Lundberg H., 1996, J. Phys. B 29, 1895
Leckrone D.S., Johansson S., Wahlgren G.M., Adelman S.J., 1993a, Phys. Scripta T47, 149
Leckrone D.S., Wahlgren G.M., Johansson S., Adelman S.J., 1993b, Peculiar versus Normal Phenomena in A-Type and Related Stars. In: Dworetsky M.M., Castelli F., Faraggiani R. (eds.) ASP Conf. Ser. 44, 42
Leckrone D.S., Johansson S.G., Wahlgren G.M., Proffitt C.R., Brage T., 1998, The Scientific Impact of the Goddard High Resolution Spectrograph. In: Brandt J.C., Ake III T.B., Petersen C.C. (eds.) ASP Conf. Ser. 143, 135
Leckrone D.S., Proffitt C.R., Wahlgren G.M., Johansson S., Brage T., 1999, AJ in press
Ralchenko Yu. V., Kramida A.E., 1995, private communication
Reader J., Acquista N., 1997, Physica Scripta 55, 310
Redfors A., 1991, A&A 249, 589
Thorne A.P., Harris C.J., Wynne-Jones I., Learner R.C.M., Cox G., 1987, J. Phys. E 20, 54
Wahlgren G.M., Adelman S.J., Robinson R.L., 1994, ApJ 434, 349
Whaling W., Carle M.T., Pitt M.L., 1993, JQSRT 50, 7